

# A neural network controller and a simple circuit of SVPWM technique to increase five-level VSC STATCOM performance during voltage sag and swell

Mohamad Milood Almelian<sup>1</sup>, Izzeldin I. Mohd<sup>2</sup>, Elhadi E. Aker<sup>3</sup>, Mohamed A. Omran<sup>4</sup>,  
Mohamed Salem<sup>5</sup>, Abu Zaharin Ahmad<sup>6</sup>, Abibaker A. Albishti<sup>7</sup>

<sup>1</sup>Department of Electrical and Electronics Engineering, Higher Institute of Sciences and Technology, Mezdah, Libya

<sup>2</sup>Faculty of Engineering, Sohar University, Sohar, Oman

<sup>3</sup>Department of Electrical and Electronics Engineering, Higher Institute of Sciences and Technology, Gharian, Libya

<sup>4</sup>College of Technical Sciences, Bani-Walid, Libya

<sup>5</sup>School of Electrical and Electronic Engineering, Universiti Sains Malaysia, Penang, Malaysia

<sup>6</sup>Faculty of Electrical and Electronics Engineering Technology, Universiti Malaysia Pahang Al-Sultan Abdullah, Pahang, Malaysia

<sup>7</sup>Department of Electrical and Electronics Engineering, Higher Institute of Sciences and Technology, Alassaba, Libya

## Article Info

### Article history:

Received Nov 29, 2022

Revised Mar 1, 2024

Accepted Mar 15, 2024

### Keywords:

Five-level VSC STATCOM

Neural network controller

Power Factor

SVPWM

Voltage magnitude

Voltage sag and swell

## ABSTRACT

The most critical disturbance faced in the electrical distribution systems is power service interruptions due to voltage sag or swell which results in economic losses on the user's side. To compensate voltage sag or swell, advanced custom power devices are used and one of such devices is the static synchronous compensation (STATCOM). This paper presents the implementation of 5-level voltage source converter (VSC) STATCOM using a neural network (NN) and a simplified space vector pulse width modulation (SVPWM) circuit. The primary objective of the NN controller and SVPWM circuit is to enhance the performance and response time of the STATCOM system, specifically in terms of improving voltage and power factor (PF) when faced with voltage sag or swell. The performance of STATCOM was examined within the context of the IEEE 3-bus system. The investigation focused on two scenarios: a single-line-to-ground fault resulting in voltage sag, and the sudden connection of a capacitive load leading to voltage swell. The findings unequivocally demonstrated the efficacy of the STATCOM with a NN controller in comparison to a conventional controller. The utilization of the NN controller resulted in notable improvements in voltage and PF within a remarkably short time frame of 0.02 seconds.

This is an open access article under the [CC BY-SA](https://creativecommons.org/licenses/by-sa/4.0/) license.



## Corresponding Author:

Mohamad Milood Almelian

Department of Electrical and Electronics Engineering, Higher Institute of Sciences and Technology

Mezdah, Libya

Email: Almalyan84@gmail.com

## 1. INTRODUCTION

The electrical grid is vulnerable to serious power quality issues as a result of system faults and the proliferation of different types of loads [1], [2]. The main issues in the distribution system are voltage sag and swell. Voltage fluctuations in the distribution system can cause electrical equipment to overheat and cause sensitive equipment to malfunction. Because of the rapid development of the power electronics industry, there is now an opportunity to improve power networks by using a flexible ac transmission system (FACTS) controller. One of the distribution level FACTS devices, the static synchronous compensator or STATCOM, has been used to correct voltage and power factor (PF) in distribution networks [3], [4]. STATCOM

performance is determined by how well and quickly error signals are compensated. As a result, the control strategy unit is the most important component of a STATCOM device. Several authors have presented STATCOM control algorithms based on traditional controllers, such as proportional integral (PI) control with sinusoidal pulse width modulation (SPWM) during voltage sag and swell. For example, Biabani *et al.* [5] presented a PI and SPWM-based control algorithm to mitigate voltage sag and harmonics, whereas [6] presented reactive power current control using STATCOM modelling based on a PI controller for voltage sag and swell compensation. Kasari *et al.* [7] describes a PI controller design for voltage stability in a distribution system using STATCOM. For the PI controller, accurate linear mathematical models are required; however, these models are tedious to obtain and usually present below-par performance when faced with parameter variations and nonlinear load fluctuations [8], [9].

Researchers have recently focused on the replacement of the conventional control systems with novel unconventional systems (such as neural network (NN) controllers). Such systems are believed to provide the best performance on several complex problems owing to their rapid dynamic response, accuracy, precision, and better steady-state and transient stability [8]. Although some studies have corrected voltage using STATCOM based on NN controllers [9], [10], there is a lack in these works in terms of training NN on tackling voltage magnitude and power factor amplitude simultaneously, resulting in unreliable STATCOM, particularly during voltage variation. Furthermore, the currently used SVPWM necessitates the calculation of switching time and sector identification, resulting in a complex circuit; however, it produces a modulation index 15% higher than SPWM, which reduces total harmonic distortion (THD) and yields a high PF [11]. As a result, this paper presented a NN-controlled cascaded 5-level voltage source converter (VSC) STATCOM with a simple SVPWM circuit for improving STATCOM performance and response time in terms of voltage and power factor improvement during voltage sag and swell.

## 2. CONFIGURATION OF IEEE 3-BUS SYSTEM WITH PROPOSED STATCOM

The STATCOM is presented in this paper in the 3-ph IEEE 3-bus test system. As shown in Figure 1, the test system includes two AC voltage supplies (G1, G2), two types of loads, and the STATCOM device circuit. The STATCOM circuit is made up of a cascaded 5-level VSC that is linked to the system via inductance ( $L_f$ ), an SVPWM scheme, and a control circuit.

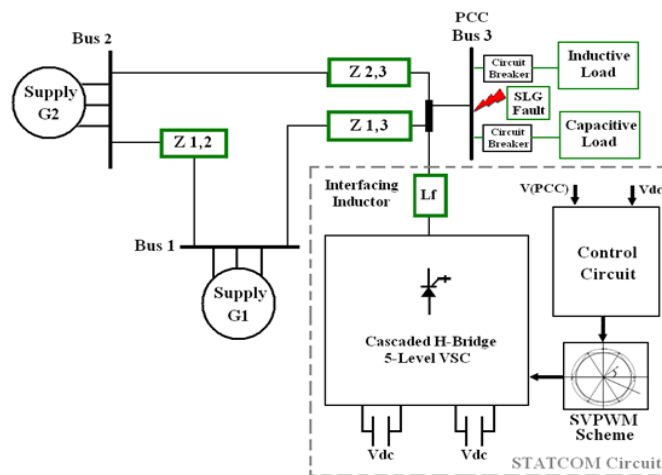


Figure 1. IEEE 3-Bus system with proposed STATCOM circuit

### 2.1. Cascaded 5-level VSC

Among multilevel VSC topologies, the cascaded multilevel VSC is the most popular because it uses the fewest components and has the most flexibility in circuit layout. The cascaded VSC topology consists of H-bridges serially connected to various DC voltage sources. The VSC structure is made up of several output voltage levels that can be easily manipulated by adding or removing H-bridges [12], [13]. Figure 2 depicts a 5-level H-bridge VSC-based STATCOM with two serially connected H-bridges (H.B1 and H.B2). In this configuration, the generated output voltage waveform is obtained by adding the individual H-bridge outputs.

The STATCOM's basic operation principle is based on two AC sources voltage (system and STATCOM) with the same frequency via coupling inductance [14]. The modulation of the amplitude of VSC

output voltage ( $V_c$ ) regulates the exchange of reactive power between STATCOM and the system [15], [16]. If the VSC output voltage amplitude surpasses the system voltage ( $V_s$ ), STATCOM produces capacitive reactive power; conversely, if it is lower than  $V_s$ , STATCOM absorbs inductive reactive power. When  $V_c$  equals  $V_s$ , the reactive power exchange between STATCOM and the system becomes zero. The reactive power ( $Q$ ) generated/absorbed by STATCOM is described as in (1), whereas the active power ( $P$ ) extracted from the system to prevent capacitor discharge is defined as in (2).

$$Q = \frac{V_s}{X_{Lf}} (V_s - V_c * \cos(\alpha)) \quad (1)$$

$$P = \frac{V_s * V_c}{X_{Lf}} \sin \alpha \quad (2)$$

Where,  $\alpha$ : Phase angle between the voltage of the VSC output and the system. The  $L_f$  that represented the L filter is determined as in (3):

$$L_f = \frac{1}{8} \times \frac{V_{dc}}{f_{sw} \times \Delta I_{Lmax}} \quad (3)$$

Here  $f_{sw}$  represents the switching frequency, and  $\Delta I_{Lmax}$  denotes the peak ripple of the maximum rated load current, equivalent to 5-20% of the rated supply current of the power system.

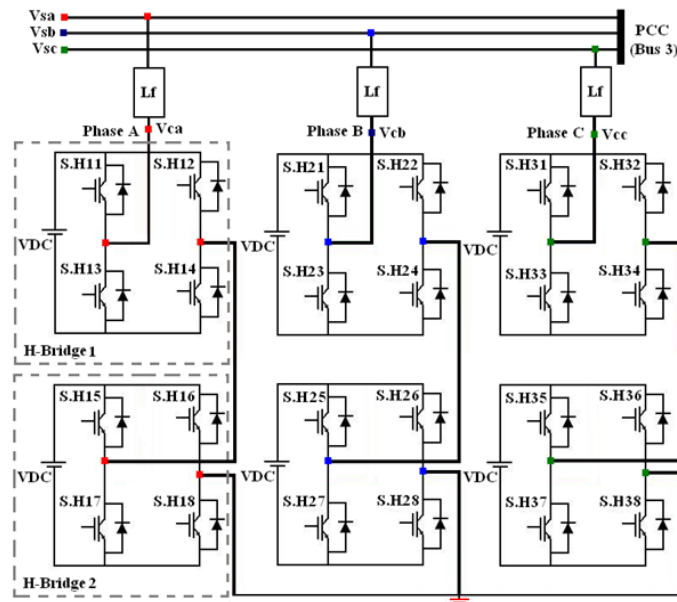


Figure 2. Cascaded H-bridge 5-level VSC

## 2.2. Simple scheme of SVPWM circuit

The utilization of the SVPWM technique in generating VSC output voltage has become prevalent in the last decade, owing to its effectiveness in reducing harmonic content and achieving higher amplitude modulation indexes compared to the SPWM technique [17]-[19]. Generally, the conventional SVPWM implementation involves several steps: identifying the sector containing the instantaneous reference space vector, mapping the identified sector to a suitable sector in the inner hexagon through coordinate transformations, determining inverter vector switching times, and utilizing switching sequence tables to select the appropriate individual vectors [11]. This section presents a straightforward and cost-effective implementation of the SVPWM technique, where the PWM switching times of the inverter legs are computed using the sampled amplitudes of the reference phase voltages. Figure 3 illustrates the SVPWM circuit, where the generation of proper pulses for each IGBT in each phase is based on the comparison of the output of the space vector circuit with the PWM signal in each H-bridge. The output signal of the SVPWM circuit by adding reference phase voltages ( $V_{ref}$ ) to the common-mode voltage ( $V_{set}$ ) can be obtained as (4) [20].

$$V_{\text{output signal of sv}} = 2/\sqrt{3} \left( V_{\text{ref}} - \frac{V_{\text{max}} + V_{\text{min}}}{2} \right) \tag{4}$$

Where  $V_{\text{max}}$  and  $V_{\text{min}}$  = maximum and minimum magnitude of the three sampled reference phase voltages, respectively.

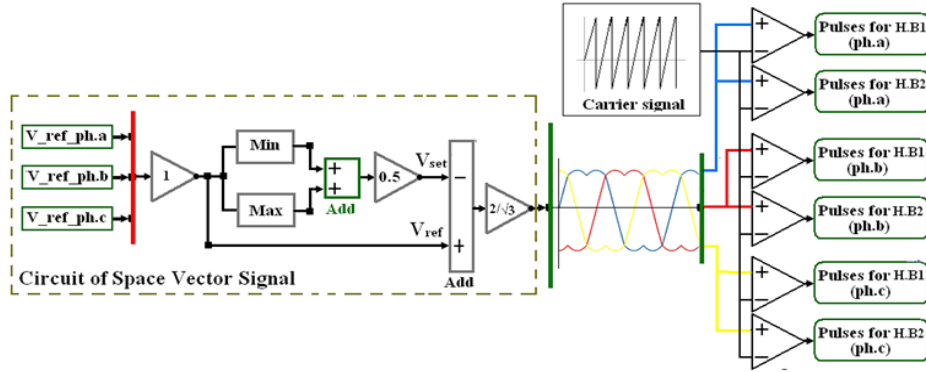


Figure 3. SVPWM scheme for cascaded 5-level VSC STATCOM

**2.3. STATCOM control circuit model**

Based on its ability to inject/absorb reactive power to/from the power system, the STATCOM control circuit is primarily used to avoid the effects of voltage sag and swell. The proposed STATCOM controller employs a direct control strategy, which allows the SVPWM (the converters' internal voltage control mechanism) to directly control the reactive output current while keeping the internal DC voltage constant [21]-[23]. The STATCOM is programmed in such a way that it should be able to change its output voltages ( $V_{ca}$ ,  $V_{cb}$ , and  $V_{cc}$ ) to deliver capacitive or inductive currents to the power system [24]. Figure 4 depicts the direct control scheme used in this study for cascaded five-level VSC STATCOM.

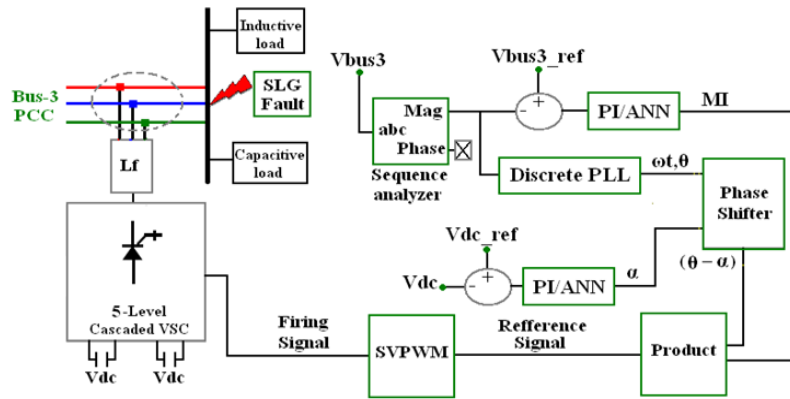


Figure 4. Proposed STATCOM control circuit strategy

In the process of designing the STATCOM control unit, a typical approach involves comparing the reference PCC voltage ( $V_{bus3\_ref}$ ) with the actual PCC voltage ( $V_{bus3}$ ). This comparison is followed by processing the difference between the two voltages through a PI/NN controller (control unit 1). The output of this controller determines the modulation index (MI) value required to maintain the voltage magnitude and power factor (PF) of the PCC at the desired level. Additionally, to facilitate a slight active power flow, the STATCOM voltage may undergo phase-shifting, achieved by adjusting the PCC voltage by a small angle ( $\alpha$ ) to keep the DC capacitor voltages constant. Another PI/NN controller (control unit 2) computes this angle based on the difference between  $V_{dc\_ref}$  and  $V_{dc}$ . Subsequently, the sinusoidal control signals are generated by inputting both the phase-locked loop (PLL) output and  $\alpha$  into the phase shifter block. These control signals, along with the modulation index (MI), are then fed into the product block, resulting in the generation

of reference signals. These reference signals are directed to the space vector pulse width modulation (SVPWM) block, responsible for producing firing pulses for each H-bridge [4]. The output voltage of the STATCOM is synchronized with the system using the PLL.

### 3. NN CONTROLLER

Artificial neural networks (ANNs) have become a prominent technological advancement in the contemporary landscape, gaining considerable attention and widespread popularity. A neural network (NN) is a sophisticated system comprised of interconnected processing elements called neurons, organized in a manner inspired by the structure of the human brain [25], [26]. The primary goal of the neural network controller is to determine suitable values for the weights and biases, the adjustable parameters within the controller's architecture, to achieve the desired output. Input to the neural network includes the error voltage at the point of common coupling (PCC) and the error voltage at the direct current (dc) link. The error is identified and subsequently backpropagated through the network, as detailed in reference [10].

This paper utilizes the Levenberg-Marquardt backpropagation (LMBP) algorithm, known for its ability to achieve rapid convergence, for the offline training of neural networks. The algorithm involves utilizing the workspace derived from the conventional PI controller to store both input and output data. The neural network architecture comprises three main components: an input layer, a hidden layer with 10 neurons, and an output layer, as illustrated in Figure 5. Regarding control unit 1, the neural network controller requires 1000 epochs for training, achieving the most optimal validation performance (VP) of  $1.48e-7$  during the sixth epoch. In the second control unit, the designated number of epochs is set to 1000, and at epoch 5, the optimal validation performance (VP) is recorded as  $1.44e-5$ .

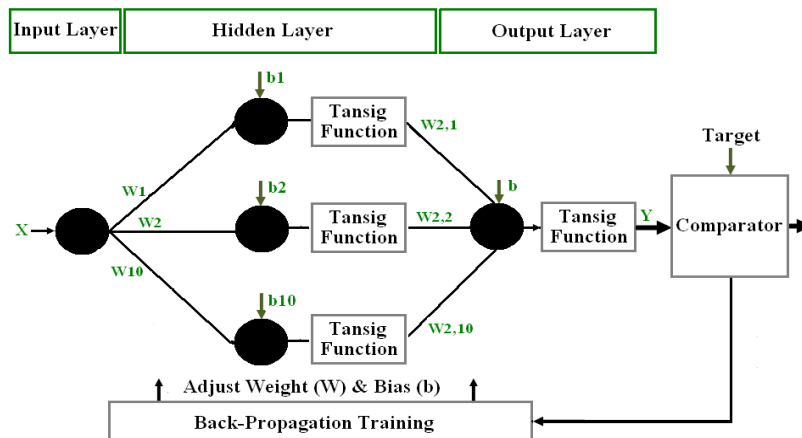


Figure 5. Structure of the NN controller

### 4. RESULTS AND DISCUSSION

The proposed STATCOM circuit was modeled in MATLAB/Simulink software, which is connected to bus-3 of the power system (specifically, the IEEE 3-bus system) as depicted in Figure 1. The model incorporates the circuit parameters provided. The alternating current (AC) voltage is set at 6.6 kilovolts line-to-line (RMS), with a frequency of 50 Hertz. The impedance of the system is determined to be 16.48 millihenries, while the resistance is measured at 0.89 ohms. The impedances between the buses, denoted as  $Z_{1,2}$ ,  $Z_{1,3}$ , and  $Z_{2,3}$ , are specified to be  $0.05+j0.2$  ohms,  $0.02+j0.1$  ohms, and  $0.036+j0.12$  ohms, respectively. Additionally, the filter inductance is determined to be 10.7 millihenries, and the direct current (DC) link voltage is set at 6 kilovolts. The load on the system is a combination of inductive and capacitive elements, with a power of 1 megawatt and a reactive power of 1 megavolt-ampere reactive (MVAR). The switching frequency of the system is set at 2 kilohertz. The proportional and integral gains ( $K_p/K_i$ ) of control unit 1 are determined to be 1 and 35, respectively, while the  $K_p/K_i$  of control unit 2 is calculated to be 0.025. The subsequent simulation outcomes demonstrate the efficacy of the cascaded 5-level VSC STSTCOM when employing a PI/NN controller to rectify voltage magnitude and power factor. The performance of the STATCOM was assessed in two scenarios: voltage sag (specifically, single line to ground (SLG) fault cases, as 80% of power system faults are attributed to SLG faults) and voltage swell.

#### 4.1. Compensation of voltage sag (SLG case)

##### 4.1.1. Voltage magnitude during voltage sag period (SLG fault case)

The connection of SLG fault at bus-3 decreased the value of the PCC voltage (0.824 pu, representing a 14.2% decrease of the nominal voltage value (0.966 pu), as seen in Figure 6). The connection of the inductive load to the IEEE 3-bus system reduced the nominal voltage to <1 pu. The voltage at the point of common coupling (PCC) was successfully restored to 0.949 per unit (pu), representing a 12.5% improvement, within a time period of 0.078 seconds. This restoration was achieved through the utilization of the Static Synchronous Compensator (STATCOM), which possesses the capability to compensate for reactive power using a PI control algorithm. Furthermore, the PCC voltage was further improved to 0.982 pu, indicating a 15.8% enhancement, within a shorter time frame of 0.02 seconds. For further details, please refer to Figures 7(a) and 7(b). In this scenario, the neural network (NN) controller demonstrated superior performance in minimizing the discrepancy between the desired value and the actual value, as compared to the PI controller unit.

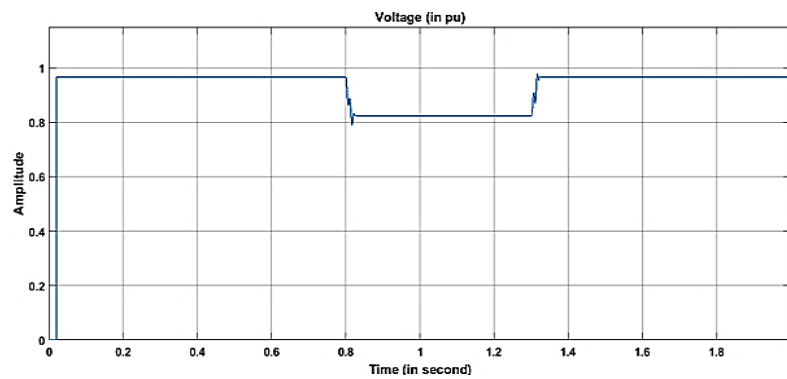
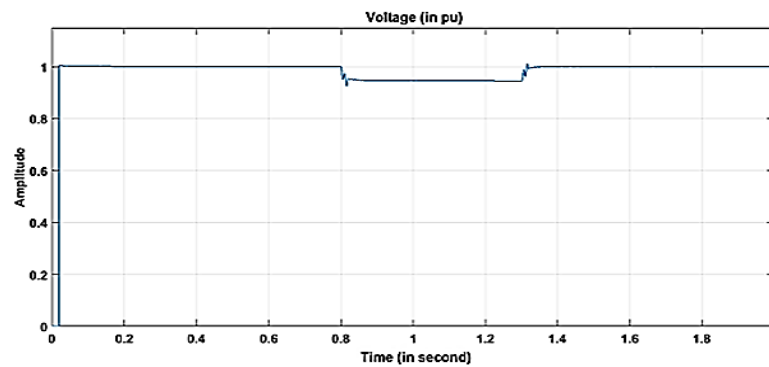
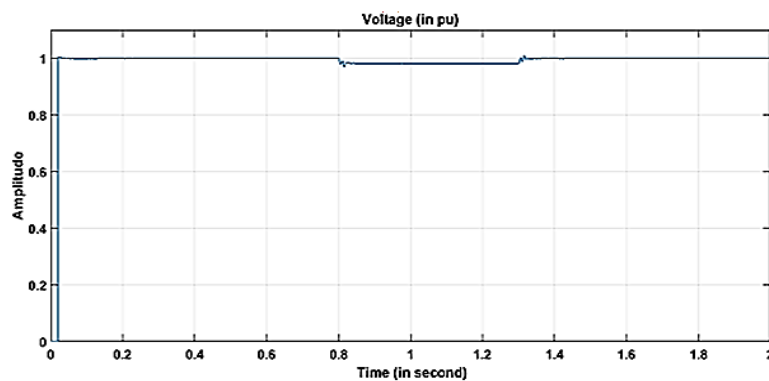


Figure 6. Voltage magnitude without the STATCOM when there is voltage sag



(a)



(b)

Figure 7. Voltage magnitude when voltage sag is present and STATCOM utilizes (a) PI and (b) NN

#### 4.1.2. Power factor during voltage sag period (SLG fault case)

The PCC voltage and current become in phase during the SLG fault period as referred to Figure 8, due to the receipt of large active power by the inductive load from the source. The PF was stabilized at 0.998 within 0.095 seconds using the STATCOM based on a PI control algorithm, as shown in Figure 9(a). STATCOM was assisted by the NN controller in maintaining a constant PF of 0.02 seconds as shown in Figure 9(b).

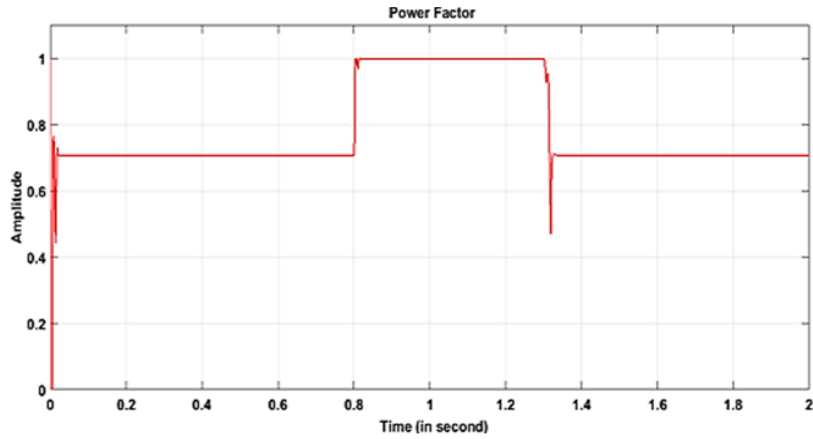
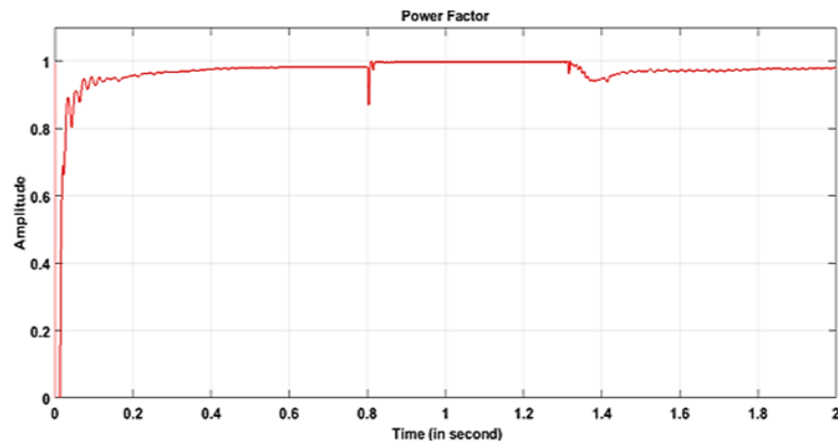
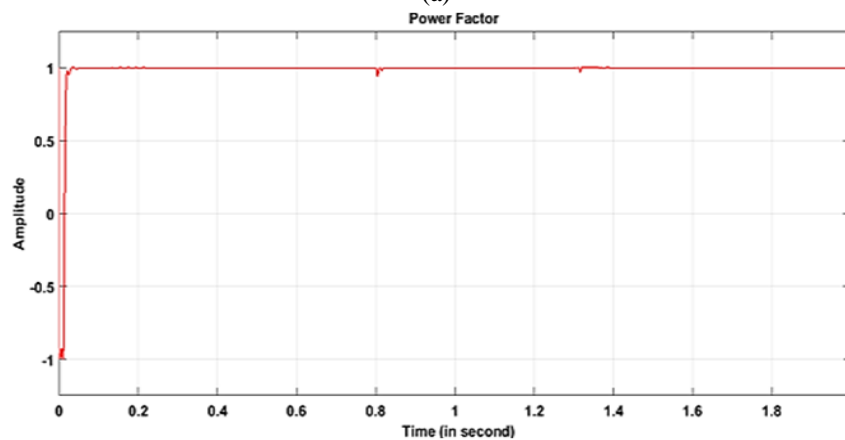


Figure 8. PF in the presence of voltage sag without the STATCOM



(a)



(b)

Figure 9. PF in the presence of voltage sag with the STATCOM based on (a) PI and (b) NN

**4.2. Compensation of voltage swell**

**4.2.1. Voltage magnitude during voltage swell period**

A sudden connection of 4MVAR at PCC yields an increased value of the voltage (1.082 pu, 12% increase) compared to 0.966 pu of the reference voltage referred to Figure 10. Figure 11(a) shows that the PI controller-based STATCOM took 0.446 seconds to correct the PCC voltage to 1.002 pu. The neural network control unit was able to decrease PCC voltage to 1.001 pu within 0.026 seconds as shown in Figure 11(b).

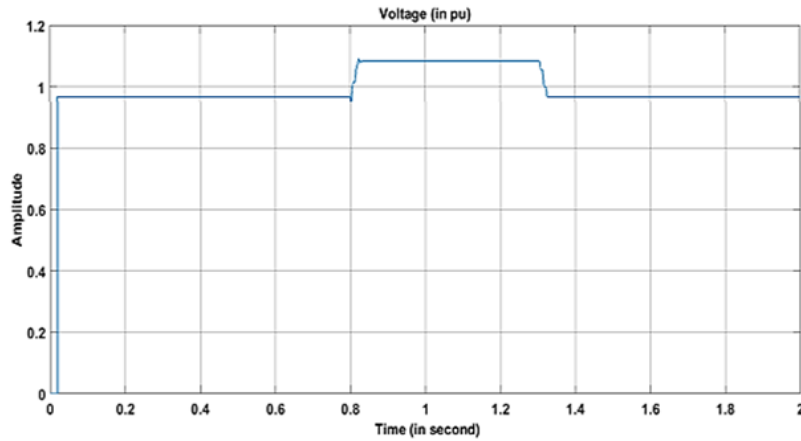
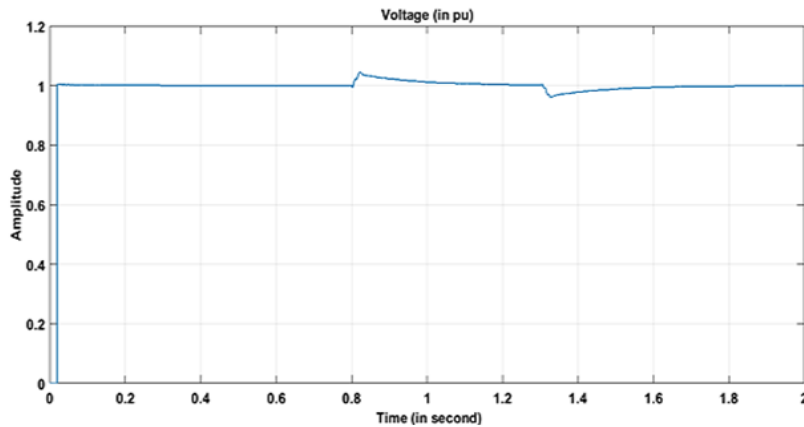
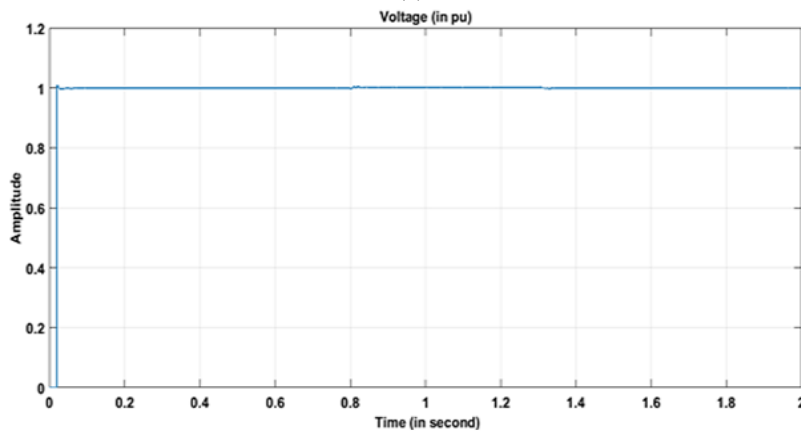


Figure 10. Voltage magnitude in the presence of voltage swell without the STATCOM



(a)



(b)

Figure 11. Voltage magnitude with STATCOM based on (a) PI and (b) NN in the presence of voltage swell

#### 4.2.2. Power factor during voltage swell

In this particular case, the current at PCC is leading in relation to the voltage. The power factor (PF) measurement, depicted in Figure 12, indicates a value of 0.56 in the absence of STATCOM. STATCOM successfully mitigated the surplus reactive power, resulting in a PF of 0.978 in 0.451 seconds when employing the PI controller. However, the utilization of NN unit for the STATCOM demonstrated enhanced performance, achieving a PF of 0.99 in 0.072 seconds, as depicted in Figures 13(a) and 13(b). The NN response time to the PI was 15.96%, indicating a significant reduction of 84.04% in time.

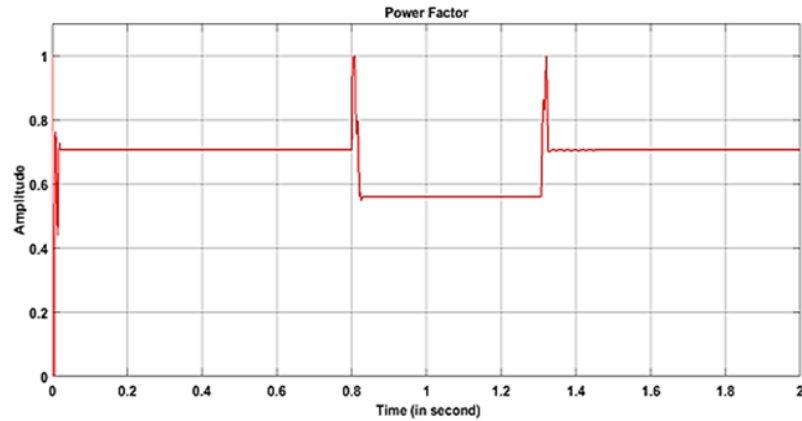
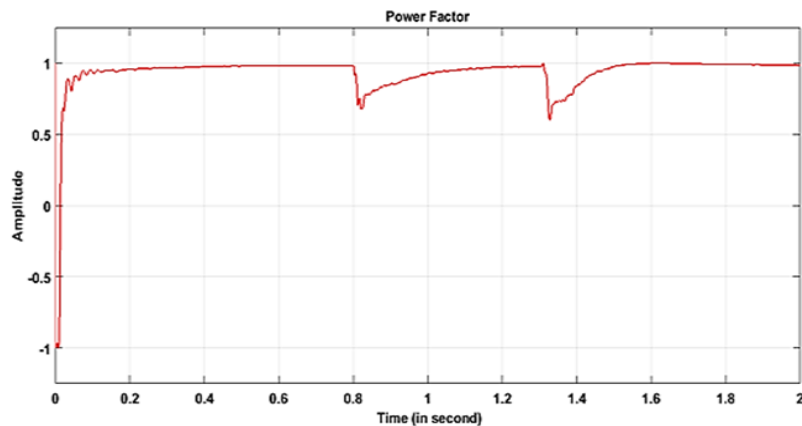
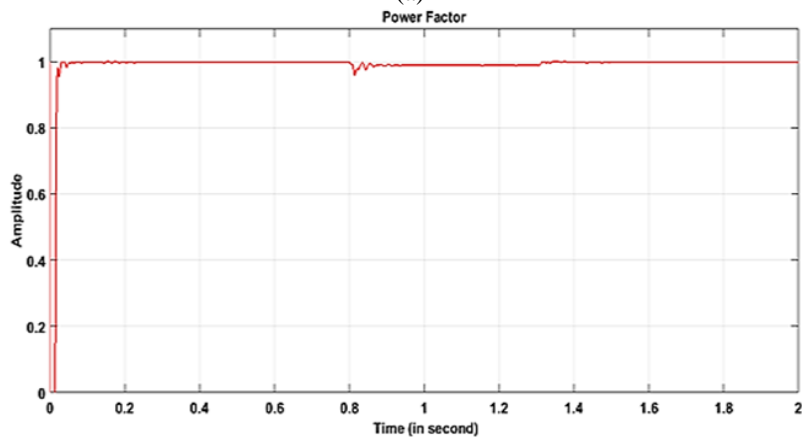


Figure 12. PF in the presence of voltage swell without the proposed STATCOM



(a)



(b)

Figure 13. PF in the presence of voltage swell with the STATCOM based on (a) PI and (b) NN

## 5. CONCLUSION

This research paper introduced a novel approach that combines a neural network control unit with a simplified space vector pulse width modulation (SVPWM) technique. The objective is to enhance the operational efficiency of a cascaded five-level voltage source converter (VSC) static synchronous compensator (STATCOM) in terms of voltage magnitude and power factor correction, particularly when faced with voltage sag and swell disturbances. The neural network-based static synchronous compensator (STATCOM) demonstrated superior performance in terms of rapid and responsive behavior, as well as accurate tracking capability, across various operational scenarios when compared to the conventional controller unit. The neural network successfully adjusted the voltage and power factor within a time frame of 1.5 cycles.

## ACKNOWLEDGEMENTS

Authors would like to express their gratitude to the Faculty of Electrical and Electronics Engineering Technology at Universiti Malaysia Pahang AI-Sultan Abdullah (UMPSA) and Faculty of Engineering at Sohar University for the invaluable support.

## REFERENCES

- [1] M. A. Omeranet *et al.*, "Utilization of filter harmonic current based on shunt HPF within the acceptable IEEE-519 Standard," in *InECCE2019: Proceedings of the 5th International Conference on Electrical, Control & Computer Engineering, Kuantan, Pahang, Malaysia, 29th July 2019*, Springer, 2020, pp. 849–858.
- [2] M. M. Almelianet *et al.*, "Improvement of Performance and Response Time of Cascaded Five-Level VSC STATCOM Using ANN Controller and SVPWM During Period of Voltage Sag," in *InECCE2019: Proceedings of the 5th International Conference on Electrical, Control & Computer Engineering, Kuantan, Pahang, Malaysia, 29th July 2019*, Springer, 2020, pp. 655–668.
- [3] M. Mahdianpoor, A. Kiyomarsi, M. Ataei, R. A. Hooshmand, and H. Karimi, "A multifunctional DSTATCOM for power quality improvement," *Turkish Journal of Electrical Engineering and Computer Sciences*, vol. 25, no. 1, pp. 172–183, 2017.
- [4] M. M. Almelianet *et al.*, "Enhancing the performance of cascaded three-level VSC STATCOM by ANN controller with SVPWM integration," *International Journal of Electrical and Computer Engineering*, vol. 9, no. 5, p. 3880, 2019.
- [5] M. A. K. A. Biabani, S. M. Ali, and A. Jawed, "Enhancement of power quality in distribution system using D-Statcom," in *2016 International Conference on Signal Processing, Communication, Power and Embedded System (SCOPES)*, IEEE, 2016, pp. 2093–2098.
- [6] M. M. Hashempour and T.-L. Lee, "Integrated power factor correction and voltage fluctuation mitigation of microgrid using STATCOM," in *2017 IEEE 3rd International Future Energy Electronics Conference and ECCE Asia (IFEEC 2017-ECCE Asia)*, IEEE, 2017, pp. 1215–1219.
- [7] P. R. Kasari, M. Paul, B. Das, and A. Chakraborti, "Analysis of D-STATCOM for power quality enhancement in distribution network," in *IEEE Region 10 Annual International Conference, Proceedings/TENCON*, 2017, pp. 1421–1426. doi: 10.1109/TENCON.2017.8228081.
- [8] C. Mittal and S. Srivastava, "Comparison of ANN and ANFIS Controller Based Hysteresis Current Control Scheme of DSTATCOM for Fault Analysis to Improve Power Quality," in *Proceedings of the International Conference on Electronics and Sustainable Communication Systems, ICESCS 2020*, 2020, pp. 149–156. doi: 10.1109/ICESCS48915.2020.9155619.
- [9] M. S. Alatshan, I. Alhamrouni, T. Sutikno, and A. Jusoh, "Improvement of the performance of statcom in terms of voltage profile using ANN controller," *International Journal of Power Electronics and Drive Systems*, vol. 11, no. 4, pp. 1966–1978, 2020, doi: 10.11591/ijpeds.v11.i4.pp1966-1978.
- [10] V. Sharma and V. K. Chandrakar, "Power Quality Enhancement by minimizing the effect of Voltage Sag in Non-linear Load Using D-STATCOM," *J Phys Conf Ser*, vol. 2325, no. 1, 2022, doi: 10.1088/1742-6596/2325/1/012019.
- [11] S. M. Muyeen, Hany. M. Hasanien, R. Takahashi, T. Murata, and J. Tamura, "Integration of space vector pulse width modulation controlled STATCOM with wind farm connected to multimachine power system," *Journal of Renewable and Sustainable Energy*, vol. 1, no. 1, 2009, doi: 10.1063/1.3049348.
- [12] S. Alatai, M. Salem, D. Ishak, M. K. Mohd Jamil, and A. Bughneda, "Design and analysis of five-level cascaded LLC resonant converter," in *PECon 2020 - 2020 IEEE International Conference on Power and Energy*, 2020, pp. 66–70. doi: 10.1109/PECon48942.2020.9314463.
- [13] S. Alatai, M. Salem, D. Ishak, A. Bughneda, M. Kamarol, and D. N. Luta, "Cascaded Multi-Level Inverter for Battery Charging-Discharging using Buck-Boost Switch," *IEACon 2021 - 2021 IEEE Industrial Electronics and Applications Conference*, pp. 108–112, 2021, doi: 10.1109/IEACon51066.2021.9654495.
- [14] A. Çetin, "Design and Implementation of a Voltage Source Converter Based Statcom for Reactive Power Compensation and Harmonic Filtering," MIDDLE EAST TECHNICAL UNIVERSITY, 2007.
- [15] B. Ismail, M. M. Naain, N. I. A. Wahab, L. J. Awal, I. Alhamrouni, and M. F. A. Rahim, "Optimal placement of DSTATCOM in distribution network based on load flow and voltage stability indices studies," in *2017 International Conference on Engineering Technology and Technopreneurship, ICE2T 2017*, 2017, pp. 1–6. doi: 10.1109/ICE2T.2017.8215973.
- [16] I. Alhamrouni, R. Ismail, M. Salem, B. Ismail, A. Jusoh, and T. Sutikno, "Integration of STATCOM and ESS for power system stability improvement," *International Journal of Power Electronics and Drive Systems*, vol. 11, no. 2, pp. 859–869, 2020, doi: 10.11591/ijpeds.v11.i2.pp868-878.
- [17] Q. M. Attique, Y. Li, and K. Wang, "A survey on space-vector pulse width modulation for multilevel inverters," *CPSS Transactions on Power Electronics and Applications*, vol. 2, no. 3, pp. 226–236, 2017.
- [18] N. Shanmugasundaram, S. P. Kumar, and E. N. Ganesh, "Modelling and analysis of space vector pulse width modulated inverter drives system using MatLab/Simulink," *International Journal of Advanced Intelligence Paradigms*, vol. 22, no. 1–2, pp. 200–213, 2022.
- [19] S. Vashishtha and K. R. Rekha, "A Survey: Space Vector PWM (SVPWM) in 3f Voltage Source Inverter (VSI)," *International Journal of Electrical & Computer Engineering (2088-8708)*, vol. 8, no. 1, 2018.
- [20] S. Tiwa, "Space vector pulse width modu," *Research Journal of Engineering Sciences*, vol. 6, no. 8, pp. 8–12, 2017.

- [21] A. Majed and Z. Salam, "Multilevel D-STATCOM for sag and swell mitigation using modulation index control," in *2015 IEEE Conference on Energy Conversion (CENCON)*, IEEE, 2015, pp. 187–192.
- [22] A. M. A. SAIF, "Direct Control of D-Statcom Based On 23-Level Cascaded Multilevel Inverter Using Harmonics Elimination Pulse Width Modulation," 2017.
- [23] K. Sayahi, A. Kadri, F. Bacha, and H. Marzougui, "Implementation of a D-STATCOM control strategy based on direct power control method for grid connected wind turbine," *International Journal of Electrical Power & Energy Systems*, vol. 121, p. 106105, 2020.
- [24] L. M. Tolbert and F. Z. Peng, "Multilevel converters for large electric drives," *IEEE Trans Ind Appl*, vol. 35, no. 1, pp. 36–44, 1999, doi: 10.1109/28.740843.
- [25] M. T. Ahmad, N. Kumar, and B. Singh, "Generalised neural network-based control algorithm for DSTATCOM in distribution systems," *IET Power Electronics*, vol. 10, no. 12, pp. 1529–1538, 2017, doi: 10.1049/iet-pel.2016.0680.
- [26] M. M. Almelian *et al.*, "Enhancement of cascaded multi-level VSC statcom performance using ANN in the presence of faults," *International Journal of Power Electronics and Drive Systems*, vol. 11, no. 2, pp. 895–906, 2020, doi: 10.11591/ijpeds.v11.i2.pp895-906.

## BIOGRAPHIES OF AUTHORS



**Mohamad Milood Almelian**    is a lecturer in Electrical and Electronic Engineering Department at Higher Institute of Sciences and Technology, Mezdah, Libya. He received his B.Eng., M.Eng. and Ph.D. degrees in Electrical Engineering from University of Gharyan, Universiti Tun Hussein Onn Malaysia (UTHM) and Universiti Malaysia Pahang Al-Sultan Abdullah (UMPSA), in 2007, 2015 and 2022, respectively. His research interests include the field of power electronics and its applications, power quality, artificial intelligence and harmonics. He can be contacted at email: Almalyan84@gmail.com.



**Izzeldin I. Mohd**    is currently holds the position of associate professor at the Faculty of Engineering in Sohar University. Prior to this role, he served as a senior lecturer at the Faculty of Electrical & Electronics Engineering Technology in Universiti Malaysia Pahang Al-Sultan Abdullah. His academic background includes a Ph.D. in Electronic and Computer Engineering obtained from Universiti Teknologi Malaysia in 2006. His research interest is primarily computer networks, with a particular focus on secure communication, secure localization, and software security, specifically in vulnerability analysis. Additionally, he maintains an interest in soft errors in deep learning system models on graphic processing units. Going forward, he continues his research in the areas of security and wireless networks, with a specific focus on cloud computing data security utilizing cryptography, artificial neural networks, and medical data management, as well as intelligent transport systems and security using blockchain technology. He can be contacted at email: iabelaziz@su.edu.om.



**Elhadi. E. Aker**    obtained bachelor of Electrical Engineering in 1986 from Assiniboine Community College Manitoba, Canada. He received master degree in Power System in 2011 from the Libyan Academy of Post Graduate Studies, Tripoli, Libya and Ph.D. in 2020 from Faculty of Engineering, Universiti Putra Malaysia (UPM). He has been serving as a lecturer at the Higher Institute of Sciences and Technology, Gharian, Libya since 2011. His research interests are in the field of power system control, switching control and smart grid applications. He can be contacted at email: hadi.aker@yahoo.com.



**Mohamed A. Omran**    received his B.Eng in Electrical Engineering from Higher institute of science and technology, Bani Walid, Libya in 2003. He received his M.Sc. and Ph.D. in Electrical Engineering from Universiti Tun Hussein Onn Malaysia (UTHM) and Universiti Malaysia Pahang Al-Sultan Abdullah (UMPSA) in 2015 and 2023, respectively. His current research interests include power electronics, power quality and harmonics. He can be contacted at email: omranmohamed346@yahoo.com.



**Mohamed Salem**    received his B.Eng. in Electrical Engineering from Elmergib University, Libya, in 2008. In 2011, he received his M.Sc. in Electrical Engineering from (UTHM), Malaysia. In August 2017, he was awarded his Ph.D. degree by the Department of Power Engineering, UTM, Malaysia. He is a member of IEEE and a registered graduate engineer (BEM) in the electrical track. Currently, he has been a senior lecturer at the School of Electrical and Electronic Engineering, USM, Penang, Malaysia since July 2018. His research interests are in DC-DC converters, renewable energy applications, and control of power electronic systems. He can be contacted at email: salemm@usm.my.



**Abu Zaharin Ahmad**    received the B.S. and M.S. degrees in Electrical Engineering from the University Technology MARA, Selangor, Malaysia, in 2001 and 2004, respectively, and the Ph.D. degree in Electrical Engineering from Chiba University, Chiba, Japan, in 2011. He was an Electrical and Instruments Engineer with Perwaja Steel Plant, Kemaman, Malaysia, before joining the Universiti Malaysia Pahang Al-Sultan Abdullah, Pahang (UMPSA), Malaysia, as a lecturer in 2005. He is currently an associate professor at the same university. His research interests are in the areas of power electronics and power system control, switching control, advanced control systems, smart grid applications, and energy harvesting. He can be contacted at email: zaharin@ump.edu.my.



**Abibaker A. Albishti**    got the B.Eng. in Electrical Engineering from Bani Walid University, Libya in 2006. He received M.S. degree in Electrical Engineering from Universiti Tun Hussein Onn Malaysia (UTHM) in 2015. Currently, he is a lecturer at the Higher Institute of Science and Technology, Alassaba, Libya. His current research interests include applications of power electronics such as in PV systems. He can be contacted at email: abobakeralbishti@gmail.com.